applied sciences

MDPI

Article

Bone Regeneration Potential of Periodontal Ligament Stem Cells in Combination with Cold Atmospheric Plasma-Pretreated Beta-Tricalcium Phosphate: An In Vivo Assessment

Maja Miletić [1,*], Nevena Puač [2], Nikola Škoro [2], Božidar Brković [3], Miroslav Andrić [3], Bogomir Bolka Prokić [4], Vesna Danilović [5], Sanja Milutinović-Smiljanić [5], Olivera Mitrović-Ajtić [6] and Slavko Mojsilović [7,*]

1 Department of Pathophysiology, School of Dental Medicine, University of Belgrade, 11000 Belgrade, Serbia
2 Institute of Physics, University of Belgrade, 11000 Belgrade, Serbia; nevena@ipb.ac.rs (N.P.); nskoro@ipb.ac.rs (N.Š.)
3 Department of Oral Surgery, School of Dental Medicine, University of Belgrade, 11000 Belgrade, Serbia; brkovic73@yahoo.com (B.B.); miroslav.andric@stomf.bg.ac.rs (M.A.)
4 Department of Surgery, Orthopedy and Ophthalmology, Faculty of Veterinary Medicine, University of Belgrade, 11000 Belgrade, Serbia
5 Department of General and Oral Histology, School of Dental Medicine, University of Belgrade, 11000 Belgrade, Serbia
6 Group for Molecular Oncology, Institute for Medical Research, University of Belgrade, 11000 Belgrade, Serbia; oliveram@imi.bg.ac.rs
7 Group for Hematology and Stem Cells, Institute for Medical Research, University of Belgrade, 11000 Belgrade, Serbia
* Correspondence: maja.miletic@stomf.bg.ac.rs (M.M.); slavko@imi.bg.ac.rs (S.M.)

Abstract: In regenerative bone tissue medicine, combining artificial bone substitutes with progenitor cells is a prospective approach. Surface modification via cold atmospheric plasma (CAP) enhances biomaterial–cell interactions, which are crucial for successful bone regeneration. Using a rabbit calvarial critical-size defect model, we assessed the use of CAP-pretreated beta-tricalcium phosphate (β-TCP), alone or with periodontal ligament stem cells (PDLSCs), for bone regeneration. Histological and histomorphometric analyses at two and four weeks revealed significantly improved bone regeneration and reduced inflammation in the CAP-treated β-TCP with PDLSCs compared to β-TCP alone. Immunohistochemical analysis also showed an increase in the bone healing markers, including bone morphogenic proteins 2 and 4, runt-related transcription factor 2, collagen-1, and osteonectin, after two and four weeks in the CAP-treated β-TCP implants with PDLSC. This in vivo study demonstrates for the first time the superior bone regenerative capacity of CAP-pretreated β-TCP seeded with PDLSCs, highlighting the therapeutic potential of this combined approach in osteoregeneration.

Keywords: bone regeneration; mesenchymal stromal cells; periodontal ligament stem cells; non-thermal atmospheric pressure plasma; tricalcium phosphate

Citation: Miletić, M.; Puač, N.; Škoro, N.; Brković, B.; Andrić, M.; Prokić, B.B.; Danilović, V.; Milutinović-Smiljanić, S.; Mitrović-Ajtić, O.; Mojsilović, S. Bone Regeneration Potential of Periodontal Ligament Stem Cells in Combination with Cold Atmospheric Plasma-Pretreated Beta-Tricalcium Phosphate: An In Vivo Assessment. *Appl. Sci.* **2024**, *14*, 16. https://doi.org/10.3390/app14010016

Academic Editor: Rossella Bedini

Received: 15 November 2023
Revised: 14 December 2023
Accepted: 15 December 2023
Published: 19 December 2023

1. Introduction

In the last few decades, several innovative therapeutic modalities have been designed to enhance bone regeneration [1]. Alloplastic bone substitutes, including beta-tricalcium phosphate (β-TCP), have osteoconductive features, meaning that they act as a scaffold for the influx of osteogenic cells, although they themselves do not have any osteoinductive or osteogenic ability [2]. Emerging bone tissue engineering strategies are based on seeding osteogenic cells onto calcium phosphate ceramic scaffolds in order to foster new bone tissue formation [3].

Among the various types of progenitor cells, mesenchymal stem cells (MSCs) represent the most frequently used population in different fields of regenerative medicine,

including bone regeneration [4,5]. Dental-derived MSCs bear similar multipotent potential and immunoregulatory capacities in comparison to bone marrow-derived MSCs, which have been traditionally applied to seed biomaterials in numerous pre-clinical and clinical studies [6–8]. The advantages of periodontal ligament stem cells (PDLSCs) over other MSCs obtained from dental tissue include easier availability, lower donor site morbidity, and lower requirements for invasive surgery [9]. It has been reported that PDLSCs have osteogenic potential and show better regeneration capability and multipotency in comparison to other subpopulations of stem cells of dental origin, which makes them a suitable alternative to BM-MSCs in terms of using cells in bone repair [9,10].

Recent research has shown that biomaterials, depending on their physicochemical properties, can modify the microenvironment of cells and trigger regulatory signals that induce the differentiation of these cells into specific cell lines. The surface characteristics of materials, such as the chemical composition, hydrophilicity, surface energy, and topography, are key factors that control the behavior of cells on the surface of biomaterials [11,12]. Various studies in recent years have shown that all these properties can be very easily modified via treatment with cold atmospheric plasma (CAP) [13–16].

Along with well-established processing using cold plasmas established at low pressures [17], cold plasmas at atmospheric pressure have paved the way for the efficient processing of different materials. CAP provides an active chemical environment close to room temperature, enabling physical and chemical interaction with the surface of materials—such as etching, deposition and activation [18]. Due to generating a diversity of reactive oxygen and nitrogen species (RONS), such as radicals, ions, excited atoms and molecules (O, OH, H_2O_2, O_3, N_2*, O_2^-, etc.), CAP is used as a prosperous technology in the medical field, with applications ranging from sterilization of medical equipment, surface modification of biomaterials, cancer treatment, to treatment of wounds and tissues, etc. [19–22]. Most of these plasma sources belong to the dielectric barrier discharge (DBD) type [23], whose main asset is a possibility to provide a large effective surface for treatment in comparison to the other plasma sources operating at atmospheric pressure. However, applications related to plasma treatments of (bio)material surfaces, i.e., bone grafting material, are infrequent and in most cases performed using low-pressure plasma systems [13,24]. Bearing in mind the potential of CAP to induce changes in the treated biomaterials [25,26], it is reasonable to believe that it can be used to enhance the regenerative potential of grafting materials, in particular when combined with MSCs.

Therefore, the aims of this in vivo study were to assess the regenerative potential of human PDLSCs seeded onto a β-TCP scaffold and to investigate if bone regeneration can be further improved via CAP pretreatment of the β-TCP.

2. Materials and Methods

2.1. Experimental Material and Cells

Periodontal ligament stem cells were isolated using the explant method, and characterized as previously described [27], from periodontal tissues of the healthy third molars extracted from patients undergoing orthodontic treatment at the Department of Oral Surgery of the School of Dental Medicine. The procedures followed the approved set of ethical guidelines published by the Ethics Committee of the Faculty of Dental Medicine, University of Belgrade (No. 36/13) after obtaining informed consent from the patients, and all the experiments were performed in accordance with the relevant guidelines and regulations. After isolation, PDLSCs were cultured in DMEM (Sigma-Aldrich, St. Luis, MO, USA) supplemented with 10% fetal bovine serum (FBS; Capricorn Scientific, Ebsdorfergrund, Germany) and 100 U/mL penicillin and 100 µg/mL streptomycin (Capricorn Scientific, Ebsdorfergrund, Germany) and passaged regularly.

As the scaffold material, synthetic β-tricalcium phosphate granules (β-TCP), size 0.5–1 mm (R.T.R. Syringe, Septodont, France), were used. For seeding onto the scaffold, the cells from passage 4 were detached using 0.05% trypsin with 1 mM EDTA (Capricorn

Scientific, Ebsdorfergrund, Germany), and 2 × 10^5 cells were seeded onto CAP-treated or untreated β-TCP granules immediately before the implantation.

2.2. Plasma Source

In this work, we used a surface dielectric barrier discharge (SDBD) system that operates in air at atmospheric pressure for the treatment of the β-TCP. A detailed electrical characterization of the DBD device that was previously used for treatments of synthetic seeds is provided in Škoro et al. [28,29]. The plasma source consisted of a glass upper part with powered and grounded segmented electrodes. It was placed above a grounded metallic surface covered with a glass dielectric plate (90 mm in diameter) that served as a sample holder (Figure 1a). The distance between the upper and lower electrode surfaces was d = 2.5 mm. In the upper part, electrodes made of 5 mm wide copper tape were placed on both sides of a 2 mm thick glass dielectric plate in an alternating manner (see Figure 1a). The copper stripes fixed to the bottom of the upper glass plate (facing the sample holder) were powered while the stripes at the top were grounded. The powered electrodes were connected to a 50 Hz sine high-voltage signal that was monitored using a high-voltage probe, while the discharge current was obtained by measuring the voltage drop on a 15 kΩ resistor. In Figure 1b, we show waveforms of the voltage and current obtained during the treatment. The spikes visible in the current signal minimum and maximum values belong to the numerous microfilaments that are formed between the powered electrode and the dielectric on the sample holder.

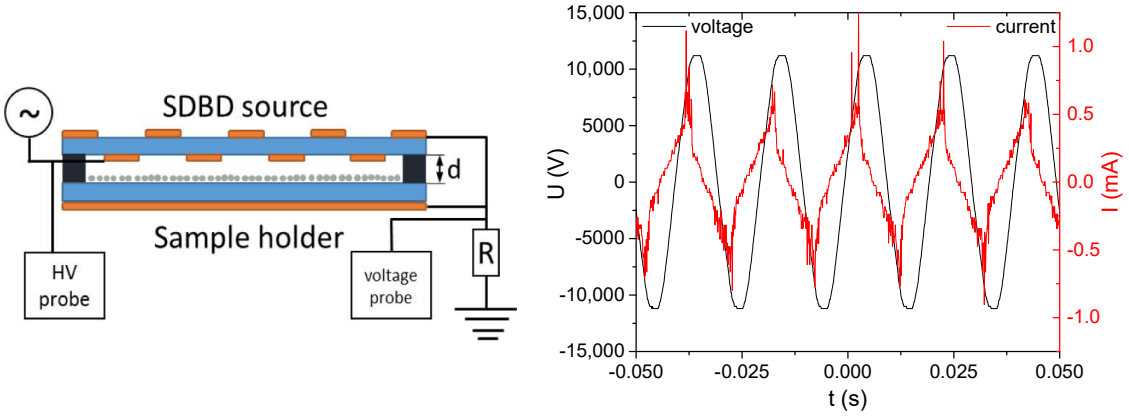

Figure 1. Experimental setup: (**a**) schematic of the surface dielectric barrier discharge (SDBD) system and (**b**) voltage and current waveforms.

For each treatment, 0.1 cm^3 of bone grafts were placed on the sample holder and equally distributed in a thin layer (less than 0.5 mm thick). The material was confined in the rectangle electrode area by using a plastic spacer to prevent dissipation of the material from active plasma volume due to drifting in the electric field. The treatment time was t = 10 min in all the treatments. We have previously used the same DBD device for the treatment of encapsulated synthetic seeds, and it was shown that the best results are obtained for the longest time, i.e., 10 min [28]. Due to the in vivo type of experiments presented in this manuscript and many study groups included, we believed that choosing the 10 min treatment as the best one based on previous experience. All the treatments were performed with identical electrical plasma parameters: VRMS = 8000 V and IRMS = 0.3 mA with mean power of around 1 W.

2.3. Animal Experiment Surgery Procedure and Study Design

The experimental procedures were approved by the Ethical Committee of the Faculty of Veterinary Medicine, University of Belgrade and the Ministry of Agriculture, Forestry and Water Management of the Republic of Serbia (No. 323-07-08477/2015-05/3), and they

were performed in accordance with Directive 2010/63/EU. Ten four-month-old Chinchilla rabbits weighing between 3.5 kg and 4.3 kg were used in this study.

Enrofloxacin (Baytril 2.5%, Bayer, Leverkusen, Germany) 10 mg/kg i.m. was used in the premedication and on five postoperative days, as well as butorphanol (Butomidor 10 mg/mL, Richter Pharma Ag, Wels, Austria) 0.5 mg/kg s.c., for pain management.

In all the animals, general anesthesia was induced via intramuscular injection of 35 mg/kg of ketamine hydrochloride (Ketamidor 10%, Richter Pharma AG, Wels, Austria) and 5 mg/kg of xylazine (Xylased 20 mg/mL, Bioveta, Ivanovice na Hané, Czech Republic). The midline incision of the scalp, created between the base of the ears and approximately 5 cm anteriorly, was performed for the full-thickness skin flap. The parietal bones were exposed after sharp subperiosteal dissection of the pericranium. Four full-thickness calvarial critical-sized defects, measuring 8 mm in diameter, were created via electrical drilling under copious saline irrigation, two of them on each side of the midline of the parietal bone (Figure 2a). A surgical template made of a sterile acrylic disk was used to ensure each defect was identical.

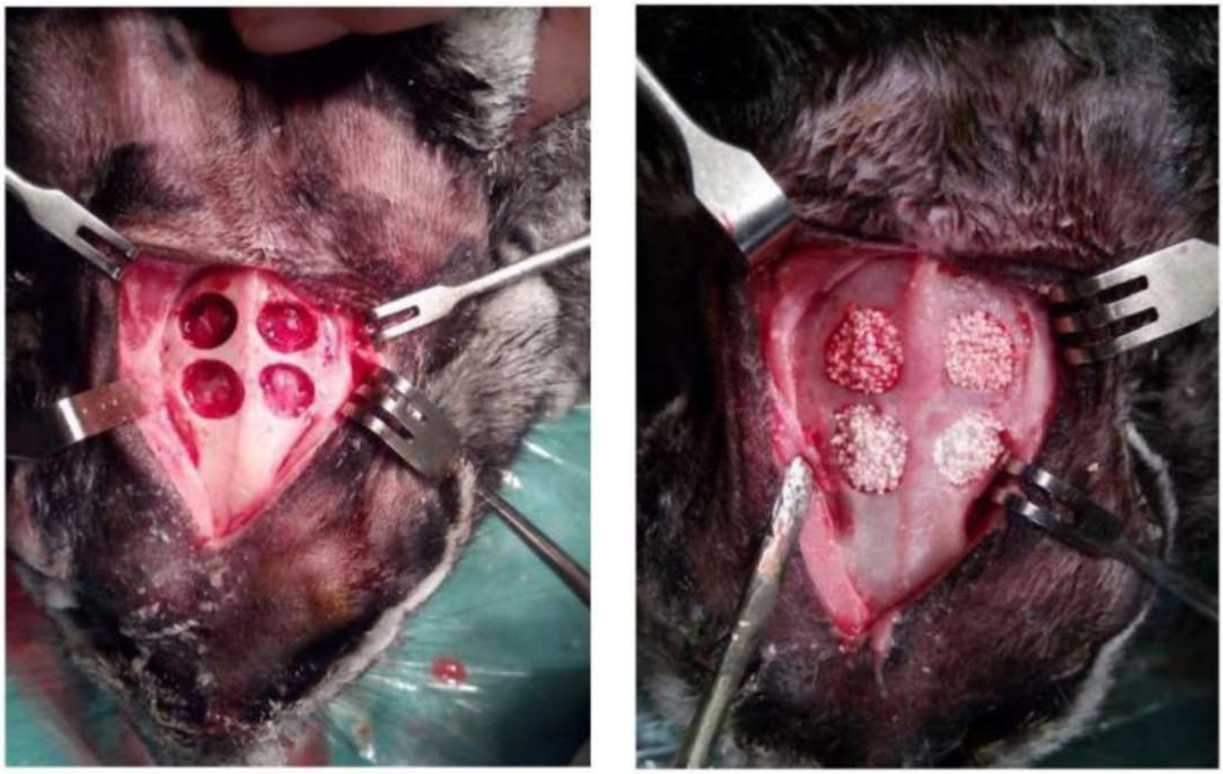

(**a**) (**b**)

Figure 2. Calvarial critical-sized defects of 8 mm of diameter in a rabbit model: (**a**) before and (**b**) after implantation.

In every rabbit, each of the four defects was randomly allocated to one of the following study groups:

Group I—defect filled with beta TCP.
Group II—defect filled with beta TCP after treatment with cold atmospheric plasma.
Group III—defect filled with beta TCP in combination with PDLSC.
Group IV—defect filled with beta TCP after treatment with cold atmospheric plasma in combination with PDLSC.

Although additional control groups would have added value to the study, we were limited by the fact that the rabbit calvaria can fit only up to four critically sized defects. In

this study, we opted for β-TCP as a base control, since it is graft material that is already used for the treatment of bone defects and has been proven to be effective.

The bone substitutes filled the bone defects from the dura to the level of marginal bone, replacing the volume of the removed bone, and the pericranium and skin were sutured in layers with absorbable sutures (Figure 2b). The surgical wound was treated once with Engemycin Spray (Intervet Productions S.r.l., Aprilia, Italy). During the postoperative animal care, the rabbits were observed twice a day until the end of the experiment. The sutures were removed 12 days after the surgery. For pain assessment, the Rabbit Grimace Scale of the National Center for the Replacement, Refinement and Reduction of animals in the research scale of Newcastle University was used.

One rabbit died postoperatively, while the remaining animals (five at two weeks and four at four weeks postoperatively) were anesthetized according to the protocol and then euthanized via intravenous application of 150 mg/kg sodium pentobarbitone. The calvarial bones were surgically removed and separated into different bone blocks according to the study groups.

2.4. Histological and Histomorphometric Analysis

The 36 bone specimens were immediately placed in 0.1 M phosphate-buffered saline solution (pH = 7.2), after which each specimen was decalcified using formic acid and embedded in paraplast blocks after a routine preparation process. Thereafter, 4 µm thick slices were cut for routine hematoxylin and eosin (HE) staining. Representative sections were selected for Masson–Goldner staining. The histological parameters were evaluated at 40× magnification under a microscope (Leitz Labor Lux S Fluorescence Microscope, Ernst Leitz Wetzlar GMBH, Wetzlar, Germany), with the exception of the inflammatory cell infiltrates, which were counted at a total magnification of 400×. The 2D images were captured at 40–400× magnification using a digital color camera (Leica DFC295, Leica Microsystems, Wetzlar, Germany). Thereafter, the images were analyzed using software (Leica University Suite, version 4.3, Leica Microsystems, Wetzlar, Germany) running on a personal computer.

The histomorphometric parameters we evaluated were the presence and area of: (1) newly formed bone tissue; (2) mineralized and non-mineralized bones (osteoids); (3) newly formed connective tissue; (4) non-resorbed bone graft particles; and (5) blood vessels. All the histomorphometric results were presented as a percentage.

The presence of an inflammatory reaction was determined based on the number of inflammatory infiltrate cells and classified as mild (0–5 cells), moderate (6–10 cells), or severe (11 or more). For each sample, three histological fields of the same surface (10,000 μm^2) per section, with a spacing of 50 µm between fields, at 400× magnification, were analyzed.

2.5. Immunohistochemical Analysis

Experimental paraffin tissue sections were cut at 5 µm, and the tissue samples were heated for 1 h at 56 °C. After that, the tissue sections were deparaffinized and rehydrated using a series of xylenes and alcohols. Endogenous peroxidase activity was blocked via the treatment of the experimental section with 3% H_2O_2 in PBS. Epitope retrieval was performed when the slides with tissue sections were heated in a microwave oven for 21 min in 10 mmol/L citrate buffer, pH = 6.0.

The experimental tissues slides were incubated overnight in humidity chambers at +4 °C with proper antibodies (dilution 1:200) against osteonectin (anti-SPARC antibody, Code: ABIN190339, Antibodies Online), runt-related transcription factor 2 (RUNX, Code: ABIN2780589), collagen type 1 (Code: ABIN 153357), bone morphogenic protein (BMP)-2 (Code: ABIN730903) and BMP-4 (Code: ABIN 223638). The immunopositivity reactive complex was imaged with a DAKO Liquid DAB+ Substrate/Chromogen System (Dako, CA, USA, Code No. K3468) and then counterstained with Mayer's hematoxylin (Merck, KGaA, Darmstadt, Germany). For the negative control, we used the tissue sections without

the primary antibodies, while for the positive control, we used the tissue sections that we already knew to express examined antibodies. For immunostaining, we used the streptavidin-biotin technique (LSAB+/HRP Kit, Peroxidase Labeling, DAKO Cytomation, Glostrup, Denmark), visualized with a DAKO Liquid DAB+ Substrate/Chromogen System (Dako, CA, USA) and counterstained with Mayer's hematoxylin (Merck KGaA, Darmstadt, Germany). The numbers of BMP-2, BMP-4, collagen-1, RUNX2 and osteonectin-positive cells were analyzed using a light microscope (Olympus AX70, Hamburg, Germany) with 40× magnification. The immunopositive cells were analyzed by defining the positive areas per every field (40× magnification) in five hotspots on every slide using ImageJ software (The National Institutes of Health, Bethesda, MD, USA), and the number of immunopositive cells was calculated for each tissue sample.

2.6. Statistics

Statistical analysis was performed using SPSS for Windows—version 18.0 software (SPSS, Inc., Chicago, IL, USA). The software G*Power 3.1.9.4 (Heinrich-Heine-Universität Düsseldorf, Düsseldorf, Germany) was used to calculate the sample size for the difference between two means, as based on the literature data, for a significance level of 0.05 and a statistical strength of 80%. All the data were presented as the mean ± SD. A two-way ANOVA was performed at a 0.05 level of significance, followed by LSD post hoc comparisons.

3. Results

3.1. Histological and Histomorphometric Analysis

Two weeks after the surgical intervention, histomorphometric analysis showed that the highest degree of bone regeneration was achieved in groups III and IV. The percentage of the total bone surface area, particularly its mineralized fraction, was statistically significantly higher in these two groups in relation to groups I and II (Table 1).

Table 1. Results of the histomorphometric analysis after 2 weeks and 4 weeks for the different study groups.

Healing Time	Group	Total Bone %	Mineralized Bone %	Non-Mineralized Bone %	Connective Tissue %	Graft Particles %	Blood Vessels %
2 weeks	I	5.55 ± 1.30	5.16 ± 1.01	0.39 ± 0.29	61.89 ± 15.00	41.85 ± 6.46	0.57 ± 0.35
	II	8.77 ± 2.80	6.77 ± 1.94	2.00 ± 0.85	42.86 ± 6.83 *	47.39 ± 5.74	0.97 ± 0.42
	III	17.52 ± 7.78 ** ##	16.93 ± 4.23 * #	0.60 ± 0.34 #	41.40 ± 4.56 *	39.84 ± 8.72	1.25 ± 0.55
	IV	23.53 ± 7.63 ** ##	21.03 ± 4.73 ** ##	2.50 ± 0.33 *	48.53 ± 2.53 #	26.99 ± 1.8 ##	0.95 ± 0.27
4 weeks	I	4.87 ± 1.40	4.17 ± 1.38	0.70 ± 0.23	48.77 ± 2.06	47.75 ± 0.71	0.61 ± 0.38
	II	11.89 ± 2.77	7.39 ± 1.81	2.44 ± 0.81	52.98 ± 3.72	36.61 ± 4.81	0.58 ± 0.26
	III	24.34 ± 7.46 **	15.33 ± 6.23 *	9.02 ± 3.43 **	47.19 ± 4.72	29.75 ± 10.53 *	0.57 ± 0.38
	IV	21.32 ± 4.82 **	14.71 ± 2.79 *	6.61 ± 2.16 *	53.51 ± 4.67	14.35 ± 1.80 *	0.99 ± 0.35

* $p < 0.05$; ** $p < 0.01$ in comparison with the control (group I); # $p < 0.05$; ## $p < 0.01$ in comparison with group II.

We did not observe a severe inflammatory reaction in any of the examined groups. In groups I and II, the inflammatory reaction was moderate. In all the tested samples of group IV and in 75% of group III, we noticed either the complete absence of inflammatory infiltrate cells or it was minimal.

Four weeks after the surgery, the total amount of newly formed bone (mineralized and non-mineralized fraction) was statistically significantly higher in groups III and IV when compared to group I. In groups III and IV, there was a reduction in the area occupied by graft particles (Table 1).

Additionally, there was a decrease in the number of inflammatory infiltrate cells compared to the two-week evaluation period, so 75% of the samples in groups I and II

had moderate inflammatory infiltrate, and 25% of the samples in these groups, as well as 100% of the samples of groups III and IV, showed the complete absence or signs of minimal inflammatory reaction.

3.2. Immunohistochemical Analysis

Two weeks after surgery, the highest number of BMP-2-positive cells was identified in group IV (Figure 3d). Immunohistochemical analysis showed a significant increase in positively stained BMP-2 cells in group IV in comparison to groups I, II, and III ($p < 0.001$) (Figure 3). After four weeks of healing, we observed a significantly higher number of BMP-2-positive cells between groups III and IV in comparison to group I ($p < 0.001$), as well as in group IV in comparison to group II ($p < 0.001$) (Figure 3).

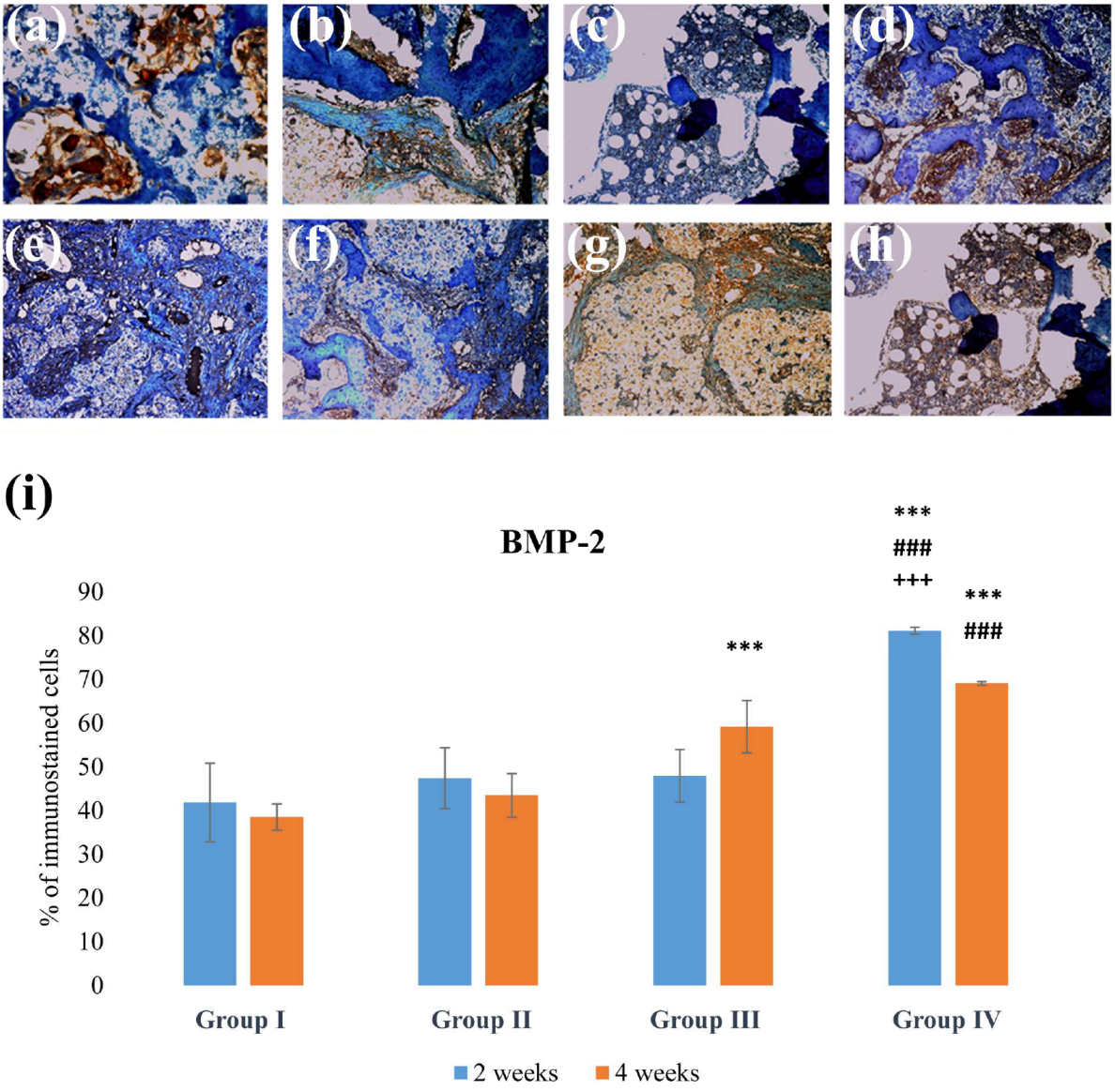

Figure 3. Immunohistochemical analysis of the BMP-2-positive cells in the defects after 2 (**a**–**d**) and 4 (**e**–**h**) weeks postoperatively: (**a**,**e**)–group I-β-TCP; (**b**,**f**)—group II-plasma-treated β-TCP; (**c**,**g**)—group III-β-TCP and PDLSCs; (**d**,**h**)–group IV-plasma-treated β-TCP and PDLSCs. (**i**) Median values of immunostaining calculated by determining the BMP-2-positive areas (brown-colored cells) are presented on the graph. The magnification in all the micrographs is 40×. ***, $p < 0.001$—compared with group I; ###, $p < 0.001$—compared with group II; +++, $p < 0.001$—compared with group III.

Two weeks postoperatively, the number of BMP-4 immunopositive cells detected in group IV (Figure 4d) was higher than in groups I, II ($p < 0.001$), and III ($p < 0.05$). A significantly higher number of BMP-4 positive cells was also detected in group III when compared to group I ($p < 0.05$) (Figure 4). After four weeks, a significantly higher number of BMP-4 positive cells was noticed in group IV in comparison to groups I ($p < 0.01$) and II ($p < 0.001$) (Figure 4).

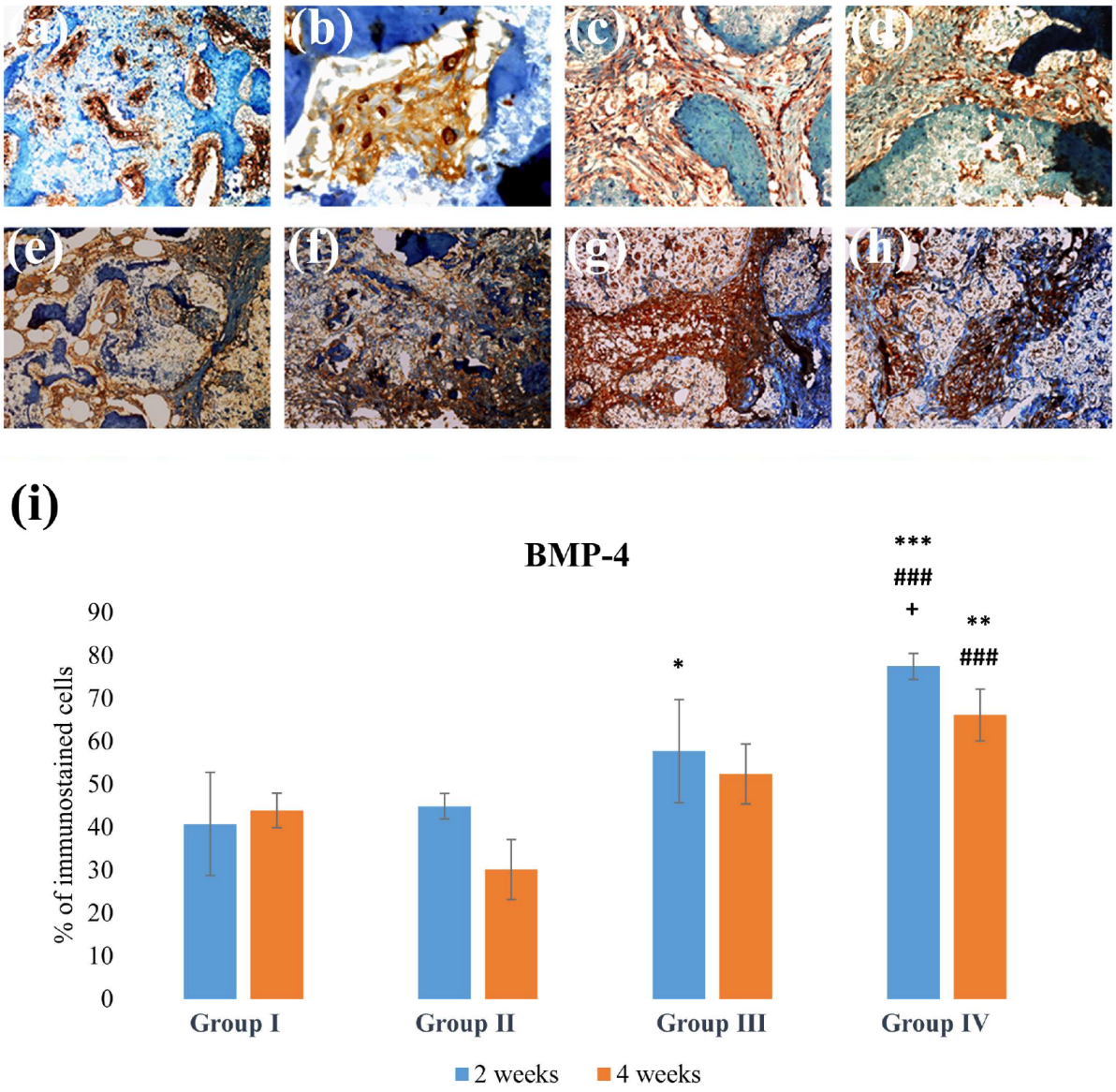

Figure 4. Immunohistochemical analysis of the BMP-4-positive cells in the defects after 2 (**a**–**d**) and 4 (**e**–**h**) weeks postoperatively: (**a**,**e**)—group I—β-TCP; (**b**,**f**)—group II—plasma-treated β-TCP; (**c**,**g**)—group III—β-TCP and PDLSCs; (**d**,**h**)—group IV—plasma-treated β-TCP and PDLSCs. (**i**) Median values of immunostaining calculated by determining the BMP-4-positive areas (brown-colored cells) are presented on the graph. The magnification in all the micrographs is 40×. * $p < 0.05$; ** $p < 0.01$; *** $p < 0.001$—compared with group I; ### $p < 0.001$—compared with group II; + $p < 0.05$—compared with group III.

Runx-2 immunopositive cells dominated in group IV, both two and four weeks after surgery (Figure 5d,h). We detected a significantly higher number of Runx-2 immunopositive cells in group IV in comparison to group I after two weeks and after four weeks in comparison to groups I and II ($p < 0.05$) (Figure 5).

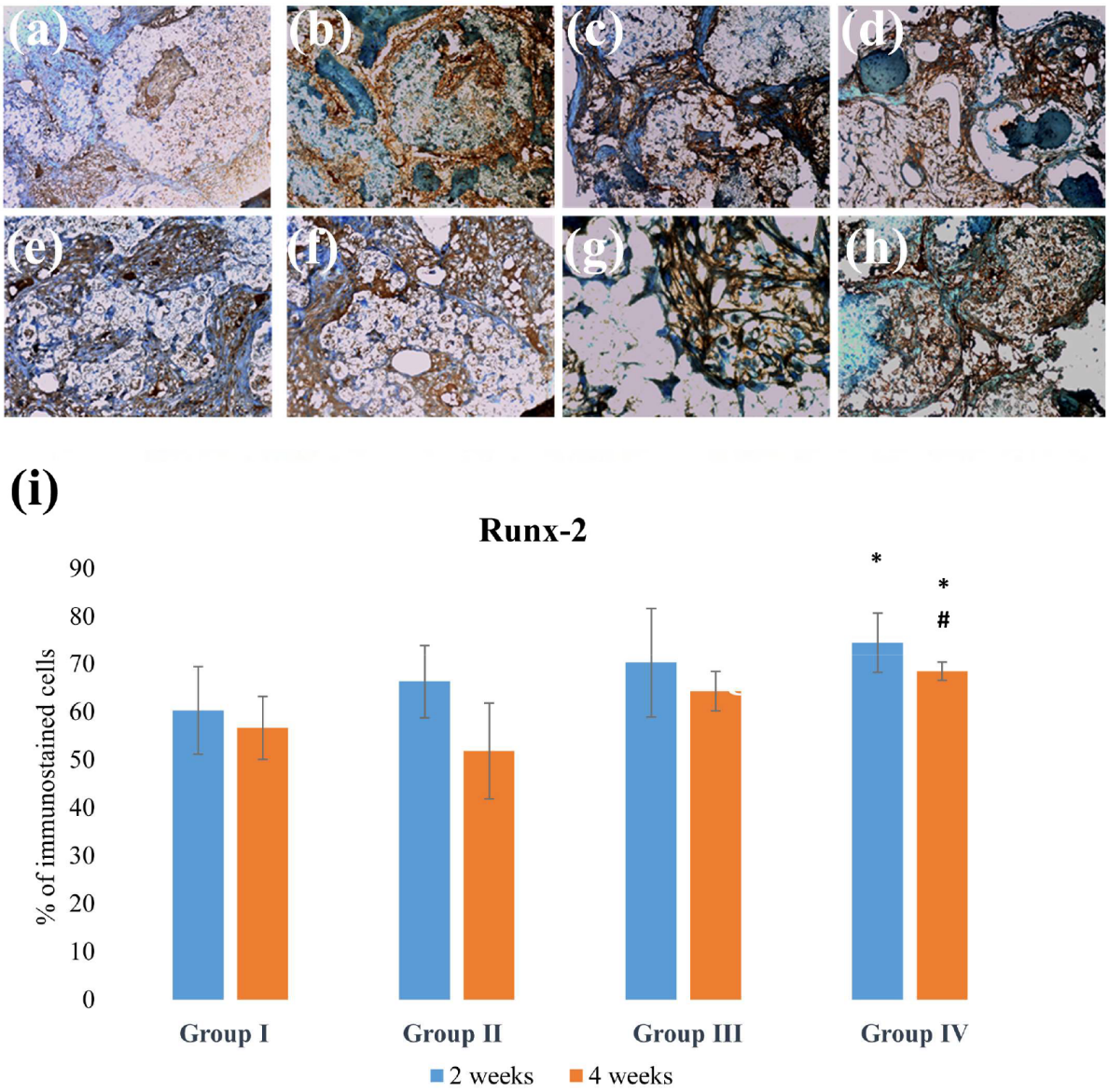

Figure 5. Immunohistochemical analysis of the Runx-2-positive cells in the defects after 2 (**a**–**d**) and 4 (**e**–**h**) weeks postoperatively: (**a**,**e**)—group I—β-TCP; (**b**,**f**)—group II—plasma-treated β-TCP; (**c**,**g**)—group III—β-TCP and PDLSCs; (**d**,**h**)—group IV—plasma-treated β-TCP and PDLSCs. (**i**) Median values of immunostaining calculated by determining the Runx-2-positive areas (brown-colored cells) are presented on the graph. The magnification in all the micrographs is 40×. * $p < 0.05$—compared with group I; # $p < 0.05$—compared with group II.

The number of collagen-1 cells, after two weeks, was significantly higher in groups II, III, and IV when compared to group I ($p < 0.001$) (Figure 6a–d).

Collagen-1 immunohistochemical staining showed that the highest number of positive cells found was four weeks after surgery in group IV (Figure 6h) and significantly more compared to group III ($p < 0.01$) (Figure 6).

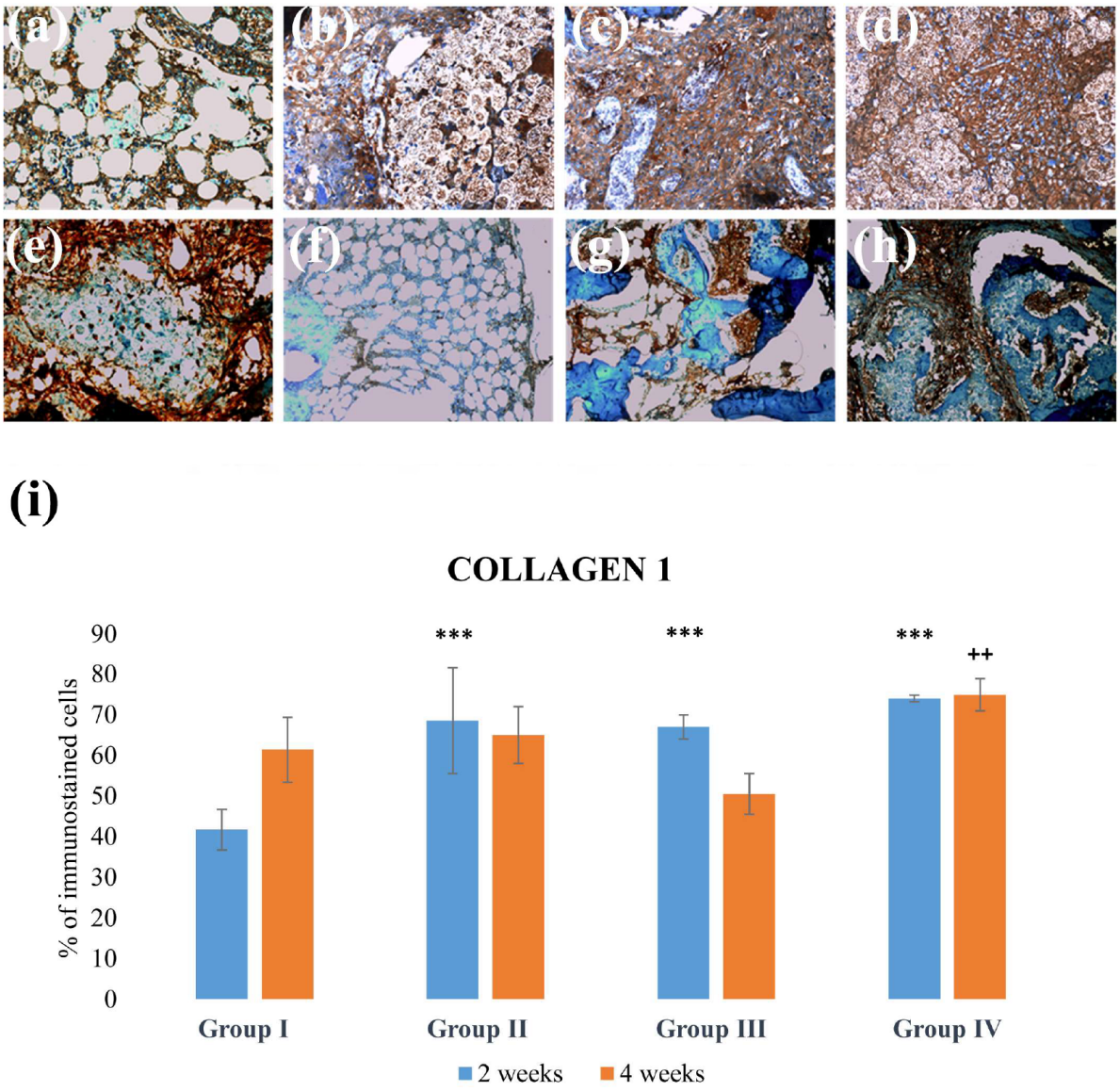

Figure 6. Immunohistochemical analysis of the collagen-1-positive cells in the defects after 2 (**a**–**d**) and 4 (**e**–**h**) weeks postoperatively: (**a**,**e**)—group I—β-TCP; (**b**,**f**)—group II—plasma-treated β-TCP; (**c**,**g**)—group III—β-TCP and PDLSCs; (**d**,**h**)—group IV—plasma-treated β-TCP and PDLSCs. (**i**) Median values of immunostaining calculated by determining the collagen-1-positive areas (brown-colored cells) are presented on the graph. The magnification in all the micrographs is 40×. *** $p < 0.001$—compared with group I; ++ $p < 0.01$—compared with group III.

Two weeks postoperatively, we did not find any significant difference in the number of osteonectin-positive cells between the four groups. However, after four weeks, the numbers of positive cells in groups II ($p < 0.001$) and IV ($p < 0.01$) were significantly higher compared to group I. Also, the combination of β-TCP, plasma and PDLSCs (group IV) significantly increased the number of osteonectin-immunopositive cells in comparison to β-TCP and PDLSCs (group III) ($p < 0.05$) (Figure 7).

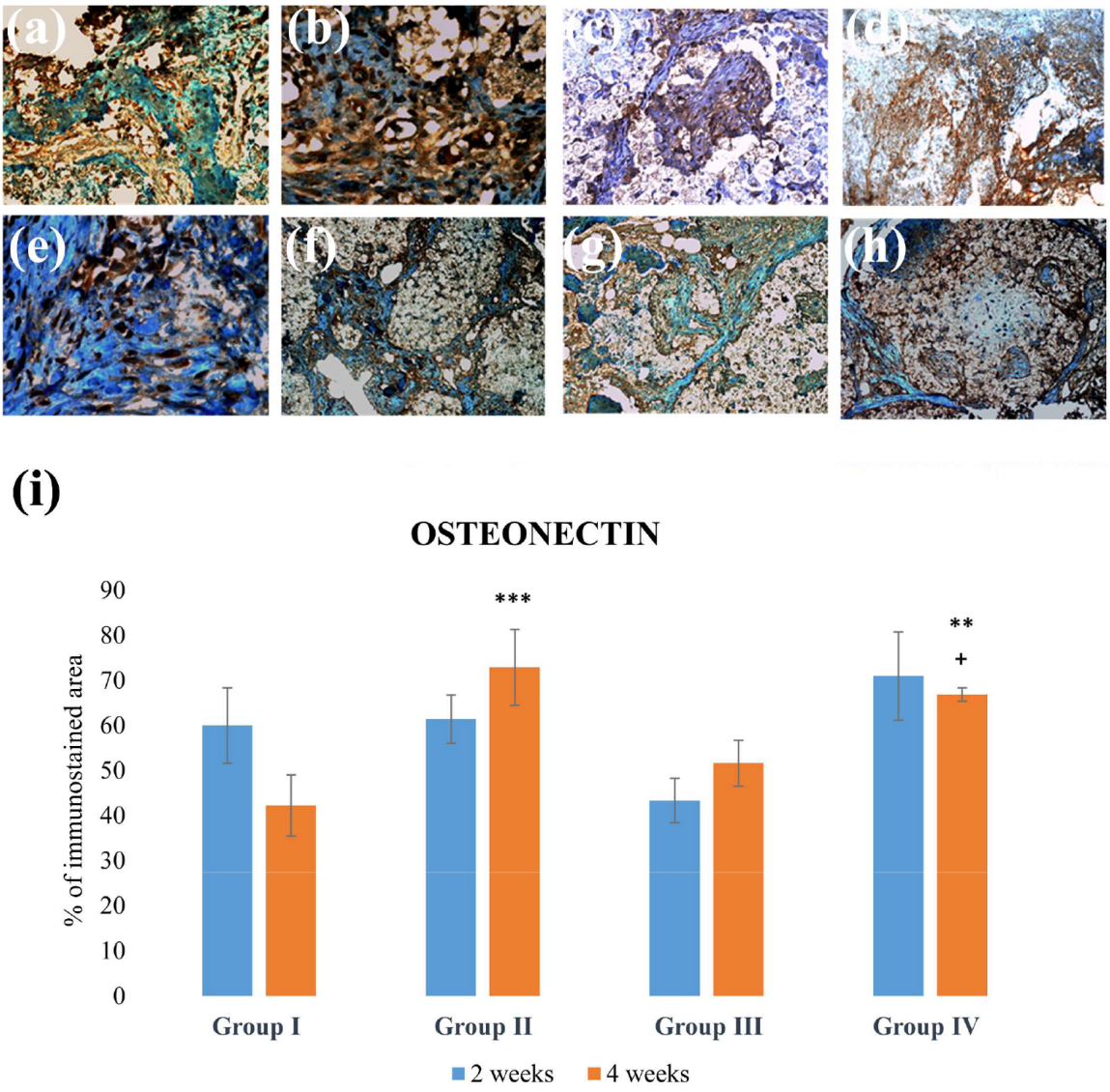

Figure 7. Immunohistochemical analysis of the osteonectin-positive cells in the defects after 2 (**a**–**d**) and 4 (**e**–**h**) weeks postoperatively: (**a**,**e**)—group I—β-TCP; (**b**,**f**)—group II—plasma-treated β-TCP; (**c**,**g**)—group III—β-TCP and PDLSCs; (**d**,**h**)—group IV—plasma-treated β-TCP and PDLSCs. (**i**) Median values of immunostaining calculated by determining the osteonectin-positive areas (brown-colored cells) are presented on the graph. The magnification in all the micrographs is 40×. ** $p < 0.01$; *** $p < 0.001$—compared with group I; + $p < 0.05$—compared with group III.

4. Discussion

According to the results of our study, histological and histomorphometric analysis demonstrated that the seeding of PDLSCs onto β-TCP, both untreated and pretreated with CAP, led to improved osteoregeneration. Our results also showed that after two weeks, most of the sites that were treated with PDLSCs had a minor or no inflammatory reaction compared to the groups without the cells, in which the inflammation was moderate up to the fourth week.

In addition to histological examination of the tissue samples, we assessed the expression of several osteogenic markers, namely BMP-2, BMP-4, collagen-1, Runx-2, and osteonectin, via immunohistochemical staining. Bone morphogenic proteins belong to the TGF-β superfamily and are involved in both initiation and terminal osteogenic differentiation [30]. Among other family members, BMP-2, -4, -6, -7, and -9 are especially important for bone formation, as they induce a signaling cascade involving the Runx-2 transcription

factor to increase osteoprogenitor cell proliferation, differentiation, and synthesis of extracellular matrix (ECM) components [31]. Collagen-1 is the main element of the bone ECM and is also expressed at the earliest stages of osteogenesis [32], while osteonectin is a glycoprotein expressed in more mature osteoblasts that binds Ca and initiates mineralization and cell–ECM interaction [33].

In general, we observed the highest percentages of immunostained cells for all the tested markers in the defects filled with CAP-treated β-TCP and PDLSCs, which additionally supports the beneficial therapeutic effects of such a combined approach on osteoregeneration. BMP-2, BMP-4, collagen-1, and Runx-2 were increased already two weeks after the implantation of the plasma-treated material seeded with the cells. This increase in the early markers of osteogenesis implies an accelerated initial phase of bone healing. Although both groups with the cells showed increased production of BMPs, the defects filled with CAP-treated β-TCP and PDLSCs showed significantly more BMP expression than with the cells seeded on untreated material. The increased presence of BMPs in lesions treated with PDLSCs may be due to the increased production of these factors by the implanted MSCs, which stay longer at the implantation site due to plasma-induced alterations in the grafting material. On the other hand, CAP-treated β-TCP alone stimulated collagen-1 production after two weeks and osteonectin production after four weeks, which is in line with their respective roles in the dynamics of bone formation. The same trend was demonstrated in the group with CAP-treated β-TCP with the cells. It is interesting that four weeks after the implantation, collagen-1 and osteonectin were expressed more in the defects filled with PDLSCs and CAP-treated β-TCP than in those filled with untreated β-TCP and cells. This could be the effect of the alteration in the hydrophilicity of the plasma-treated surface. Even though a few studies have investigated the influence of plasma-treated biomaterial surfaces on pro-osteogenic cell activities in vitro [15,34,35], to the best of our knowledge, there is no research that has explored the in vivo effects of surface-modified calcium phosphate biomaterials in combination with MSCs on bone regeneration. Future works will need to investigate in more depth the origin of the secreted proteins and the exact role that human MSCs play in this process.

The positive interactions of biomaterials and cells are crucial for successful bone regeneration. Research have shown that the surface characteristics of calcium phosphates, like the chemical composition, molecular weight, and surface properties, including the hydrophilicity and topography, can positively affect stem cell functions such as the adhesion, proliferation and differentiation [36,37]. The power deposited in the CAP used for the treatment of the β-TCP samples was kept at the level of 1 W, which means that most likely there was no erosion of the treated material. The CAPs have an important characteristic in that they operate at room temperature while having a rich gas-phase chemistry due to the electrons with much higher energy than the neutral gas, ions, and other species. This leads to the production of reactive oxygen and nitrogen species (RONS): superoxide anion (O_2^-), hydroxyl radicals (OH), oxygen atoms (O), hydrogen peroxide (H_2O_2), ozone (O_3), nitrite (NO_2), nitric oxide (NO), nitrate (NO_3), peroxynitrite (ONOO-), etc. [38–40]. Broadly speaking, the production rates and amounts of RONS are connected to the deposited power in the plasma, to the presence of surrounding gas that is diffused in the plasma working gas, the geometry of the discharge and the type of target. In our case, the RONS created in the plasma gas phase are in contact with the surface of the β-TCP samples during the treatments, and their mutual interaction leads to changes in the material surface chemistry. One can expect that the wettability is increased as well as the surface energy of the plasma treated samples of β-TCP [24,41]. This can lead to better adhesion of the cells, with the result of better bone regeneration. The influence of CAP treatment on materials is limited to the surface and surface chemistry. During plasma treatment, C-C and C-H bonds are usually broken and carbon content decreases with the increase in oxygen content. Beutel et al. confirmed the increase in the oxygen and calcium percentages and decrease in the carbon presence in the surface chemistry of β-TCP scaffolds when treated by argon CAP [24].

Canullo et al. have demonstrated that the protein adsorption and murine osteoblasts adhesion are increased by argon plasma surface modification of hydroxyapatite (HA) and calcium phosphate ceramics [35]. Choi et al. also showed that following the treatment of HA/β-TCP with nitrogen and air CAP, the attachment and proliferation of MC3T3 mouse osteoblasts were increased [15]. This can be achieved by increasing the hydrophilicity of the scaffold surface. It has been reported that when a surface is treated with CAP, the carbon levels decrease, whereas the levels of oxygen functional groups increase, resulting in a more polar and hydrophilic surface [13–15]. The hydrophilicity of a surface is essential for the adsorption of ECM proteins and hence the adhesion of cells via cell–ECM interactions [42]. In addition, it has been reported that hydrophilic surfaces contribute to the adhesion and proliferation of osteoblasts while simultaneously promoting the maturation and differentiation of bone precursor cells, which leads to the creation of a pro-osteogenic microenvironment [43]. On the other hand, macrophage activity is also affected by the hydrophilicity and microporosity of surfaces [44,45]. The increased surface energy of hydrophilic surfaces enhances the release of anti-inflammatory markers by macrophages and modulates their polarization to anti-inflammatory phenotypes [46,47]. It has also been shown that the surface topography influences the gene expression and cytokine secretion profile of MSCs and enhances their osteogenic differentiation capacity [48,49].

The implanted MSCs do not survive long at the implantation site but initiate the bone regeneration process by recruiting host MSCs and osteoprogenitors, resolving inflammation by modulating the immune response and initiating reparatory M2 macrophage polarization [50,51]. MSCs also suppress Th1 and cytotoxic T cell proliferation and function, favoring Th2 and Treg cell polarization, inhibit NK cell cytotoxicity and induce tolerogenic DC generation. This immunosuppressive effect is crucial for terminating the inflammatory phase and moving to the regenerative phase, thereby avoiding chronic inflammation, which is detrimental to any tissue regeneration [44]. On the other hand, M2 macrophages, and osteoclasts generated by phagocytosis and creating an acidic environment, lead to the resorption of calcium phosphate materials and release of calcium and phosphate ions [52], which contribute to MSC osteogenic differentiation and mineralization [53]. Previous studies have shown that macrophage recruitment to an implanted calcium phosphate is significantly enhanced when the calcium phosphate scaffold is seeded with MSCs [44,51,54]. Based on these studies and our results, we can consider surface modification of β-TCP by CAP as a way to increase the adhesion and interaction of MSCs with the material, as well as the surrounding host tissue and cells, leading to the transition from a pro-inflammatory to a pro-reparatory microenvironment.

5. Conclusions

This study showed that CAP-pretreated β-TCP in combination with PDLSCs had significantly higher bone regeneration capacity and decreased inflammatory reaction compared to β-TCP alone. Even though this study has its limitations, such as a lack of physicochemical analysis of the CAP-treated material, our findings suggest that treatment with CAP could be a relatively simple, inexpensive, and effective method of treating β-TCP that improves the interaction of the material with stem cells, thus enhancing bone regeneration. This research opens up new perspectives on the development of advanced methods in MSC-based bone tissue engineering strategies supported by CAP technology to augment the healing of difficult bone lesions.

Author Contributions: Conceptualization, M.M. and S.M.; methodology, M.M, N.P., N.Š., B.B., M.A., B.B.P. and S.M.; validation, M.M. and S.M.; formal analysis, S.M.-S. and O.M.-A.; investigation, M.M., N.P., N.Š., B.B., M.A., B.B.P., V.D., S.M.-S., O.M.-A. and S.M.; resources, M.M. and N.P.; data curation, M.M., S.M.-S., O.M.-A. and S.M.; writing—original draft preparation, M.M., N.P., N.Š., M.A., B.B.P., S.M.-S., O.M.-A. and S.M.; writing—review and editing, M.M., N.P., N.Š., M.A. and S.M.; visualization, M.M., N.P., N.Š., O.M.-A. and S.M.; supervision, M.M.; project administration, M.M., N.P. and S.M.; funding acquisition, M.M. and N.P. All authors have read and agreed to the published version of the manuscript.

Funding: This research was funded by the Ministry of Science, Technological Development and Innovations of the Republic of Serbia, contract numbers 451-03-47/2023-01/200129 (MM, BB, MA, SMS, VD), 451-03-47/2023-01/200015 (SM, OMA), 451-03-68/2023-14/200024 (NP, NS), 451-03-47/2023-01/200143 (BBP).

Institutional Review Board Statement: This study was conducted in accordance with the Declaration of Helsinki, and it was approved by the Ethics Committee of the Faculty of Dental Medicine, University of Belgrade (No. 36/13 and date of approval). The animal study protocol was approved by the Ethical Committee of the Faculty of Veterinary Medicine, University of Belgrade, and the Ministry of Agriculture, Forestry and Water Management of the Republic of Serbia (No. 323-07-08477/2015-05/3).

Informed Consent Statement: Informed consent was obtained from all the subjects involved in the study.

Data Availability Statement: The data presented in this study are available on request from the corresponding author.

Conflicts of Interest: The authors declare no conflict of interest.

References

1. Manzini, B.M.; Machado, L.M.R.; Noritomi, P.Y.; DA Silva, J.V.L. Advances in Bone Tissue Engineering: A Fundamental Review. *J. Biosci.* **2021**, *46*, 17. [CrossRef]
2. Fukuba, S.; Okada, M.; Nohara, K.; Iwata, T.; Iwata, T. Alloplastic Bone Substitutes for Periodontal and Bone Regeneration in Dentistry: Current Status and Prospects. *Materials* **2021**, *14*, 1096. [CrossRef]
3. Li, Y.; Jiang, T.; Zheng, L.; Zhao, J. Osteogenic Differentiation of Mesenchymal Stem Cells (MSCs) Induced by Three Calcium Phosphate Ceramic (CaP) Powders: A Comparative Study. *Mater. Sci. Eng. C* **2017**, *80*, 296–300. [CrossRef]
4. Saeed, H.; Ahsan, M.; Saleem, Z.; Iqtedar, M.; Islam, M.; Danish, Z.; Khan, A.M. Mesenchymal Stem Cells (MSCs) as Skeletal Therapeutics–an Update. *J. Biomed. Sci.* **2016**, *23*, 41. [CrossRef]
5. Mushahary, D.; Spittler, A.; Kasper, C.; Weber, V.; Charwat, V. Isolation, Cultivation, and Characterization of Human Mesenchymal Stem Cells: hMSC. *Cytometry* **2018**, *93*, 19–31. [CrossRef]
6. Jin, Y.-Z.; Lee, J.H. Mesenchymal Stem Cell Therapy for Bone Regeneration. *Clin. Orthop. Surg.* **2018**, *10*, 271. [CrossRef]
7. Ruan, S.; Deng, J.; Yan, L.; Huang, W. Composite Scaffolds Loaded with Bone Mesenchymal Stem Cells Promote the Repair of Radial Bone Defects in Rabbit Model. *Biomed. Pharmacother.* **2018**, *97*, 600–606. [CrossRef]
8. Blanco, J.F.; Villarón, E.M.; Pescador, D.; da Casa, C.; Gómez, V.; Redondo, A.M.; López-Villar, O.; López-Parra, M.; Muntión, S.; Sánchez-Guijo, F. Autologous Mesenchymal Stromal Cells Embedded in Tricalcium Phosphate for Posterolateral Spinal Fusion: Results of a Prospective Phase I/II Clinical Trial with Long-Term Follow-Up. *Stem Cell Res. Ther.* **2019**, *10*, 63. [CrossRef]
9. Kämmerer, P.W.; Scholz, M.; Baudisch, M.; Liese, J.; Wegner, K.; Frerich, B.; Lang, H. Guided Bone Regeneration Using Collagen Scaffolds, Growth Factors, and Periodontal Ligament Stem Cells for Treatment of Peri-Implant Bone Defects *In Vivo*. *Stem Cells Int.* **2017**, *2017*, 3548435. [CrossRef]
10. Zhang, Y.; Xing, Y.; Jia, L.; Ji, Y.; Zhao, B.; Wen, Y.; Xu, X. An In Vitro Comparative Study of Multisource Derived Human Mesenchymal Stem Cells for Bone Tissue Engineering. *Stem Cells Dev.* **2018**, *27*, 1634–1645. [CrossRef]
11. Cui, H.; Wang, X.; Wesslowski, J.; Tronser, T.; Rosenbauer, J.; Schug, A.; Davidson, G.; Popova, A.A.; Levkin, P.A. Assembly of Multi-Spheroid Cellular Architectures by Programmable Droplet Merging. *Adv. Mater.* **2021**, *33*, 2006434. [CrossRef] [PubMed]
12. Tirrell, M.; Kokkoli, E.; Biesalski, M. The Role of Surface Science in Bioengineered Materials. *Surf. Sci.* **2002**, *500*, 61–83. [CrossRef]
13. Choy, C.S.; Lee, W.F.; Lin, P.Y.; Wu, Y.-F.; Huang, H.-M.; Teng, N.-C.; Pan, Y.-H.; Salamanca, E.; Chang, W.-J. Surface Modified β-Tricalcium Phosphate Enhanced Stem Cell Osteogenic Differentiation in Vitro and Bone Regeneration in Vivo. *Sci. Rep.* **2021**, *11*, 9234. [CrossRef]
14. Moriguchi, Y.; Lee, D.-S.; Chijimatsu, R.; Thamina, K.; Masuda, K.; Itsuki, D.; Yoshikawa, H.; Hamaguchi, S.; Myoui, A. Impact of Non-Thermal Plasma Surface Modification on Porous Calcium Hydroxyapatite Ceramics for Bone Regeneration. *PLoS ONE* **2018**, *13*, e0194303. [CrossRef]
15. Choi, Y.-R.; Kwon, J.-S.; Song, D.-H.; Choi, E.H.; Lee, Y.-K.; Kim, K.-N.; Kim, K.-M. Surface Modification of Biphasic Calcium Phosphate Scaffolds by Non-Thermal Atmospheric Pressure Nitrogen and Air Plasma Treatment for Improving Osteoblast Attachment and Proliferation. *Thin Solid. Film.* **2013**, *547*, 235–240. [CrossRef]
16. Wagner, G.; Eggers, B.; Duddeck, D.; Kramer, F.-J.; Bourauel, C.; Jepsen, S.; Deschner, J.; Nokhbehsaim, M. Influence of Cold Atmospheric Plasma on Dental Implant Materials—An in Vitro Analysis. *Clin. Oral. Investig.* **2022**, *26*, 2949–2963. [CrossRef]
17. Makabe, T.; Petrovic, Z.L. *Plasma Electronics*; CRC Press: Boca Raton, FL, USA, 2006; ISBN 978-1-4200-1227-9.
18. Keidar, M.; Weltmann, K.-D.; Macheret, S. Fundamentals and Applications of Atmospheric Pressure Plasmas. *J. Appl. Phys.* **2021**, *130*, 80401. [CrossRef]
19. Mumtaz, S.; Khan, R.; Rana, J.N.; Javed, R.; Iqbal, M.; Choi, E.H.; Han, I. Review on the Biomedical and Environmental Applications of Nonthermal Plasma. *Catalysts* **2023**, *13*, 685. [CrossRef]

20. Moisan, M.; Barbeau, J.; Crevier, M.-C.; Pelletier, J.; Philip, N.; Saoudi, B. Plasma Sterilization. *Methods Mech. Pure Appl. Chem.* **2002**, *74*, 349–358. [CrossRef]
21. Lu, X.; Reuter, S.; Laroussi, M.; Liu, D. *Nonequilibrium Atmospheric Pressure Plasma Jets: Fundamentals, Diagnostics, and Medical Applications*, 1st ed.; CRC Press: Boca Raton, FL, USA, 2019; ISBN 978-0-429-05366-5.
22. Von Woedtke, T.; Reuter, S.; Masur, K.; Weltmann, K.-D. Plasmas for Medicine. *Phys. Rep.* **2013**, *530*, 291–320. [CrossRef]
23. Becker, K.H.; Kogelschatz, U.; Schoenbach, K.H.; Barker, R.J. (Eds.) *Non-Equilibrium Air Plasmas at Atmospheric Pressure*, 1st ed.; CRC Press: Boca Raton, FL, USA, 2005; ISBN 978-0-429-17508-4.
24. Beutel, B.G.; Danna, N.R.; Gangolli, R.; Granato, R.; Manne, L.; Tovar, N.; Coelho, P.G. Evaluation of Bone Response to Synthetic Bone Grafting Material Treated with Argon-Based Atmospheric Pressure Plasma. *Mater. Sci. Eng. C* **2014**, *45*, 484–490. [CrossRef] [PubMed]
25. Trimukhe, A.M.; Pandiyaraj, K.N.; Tripathi, A.; Melo, J.S.; Deshmukh, R.R. Plasma Surface Modification of Biomaterials for Biomedical Applications. In *Advances in Biomaterials for Biomedical Applications*; Tripathi, A., Melo, J.S., Eds.; Advanced Structured Materials; Springer: Singapore, 2017; Volume 66, pp. 95–166. ISBN 978-981-10-3327-8.
26. Cvelbar, U.; Canal, C.; Hori, M. Plasma-Inspired Biomaterials. *J. Phys. D Appl. Phys.* **2017**, *50*, 40201. [CrossRef]
27. Miletic, M.; Mojsilovic, S.; Okic-Djordjevic, I.; Kukolj, T.; Jaukovic, A.; Santibacez, J.F.; Jovcic, G.; Bugarski, D. Mesenchymal Stem Cells Isolated from Human Periodontal Ligament. *Arch. Biol. Sci.* **2014**, *66*, 261–271. [CrossRef]
28. Škoro, N.; Živković, S.; Jevremović, S.; Puač, N. Treatment of Chrysanthemum Synthetic Seeds by Air SDBD Plasma. *Plants* **2022**, *11*, 907. [CrossRef] [PubMed]
29. Bajić, M.; Škoro, N.; Puač, N.; Petrović, Z.L. Electrical Characterisation of the Surface DBD Operating in Air. In Proceedings of the SPIG 2018, Belgrade, Serbia, 28 August–1 September 2018; p. 230.
30. Salazar, V.S.; Gamer, L.W.; Rosen, V. BMP Signalling in Skeletal Development, Disease and Repair. *Nat. Rev. Endocrinol.* **2016**, *12*, 203–221. [CrossRef] [PubMed]
31. Millan, C.; Vivanco, J.F.; Benjumeda-Wijnhoven, I.M.; Bjelica, S.; Santibanez, J.F. Mesenchymal Stem Cells and Calcium Phosphate Bioceramics: Implications in Periodontal Bone Regeneration. In *Cell Biology and Translational Medicine, Volume 3*; Turksen, K., Ed.; Advances in Experimental Medicine and Biology; Springer International Publishing: Cham, Switzerland, 2018; Volume 1107, pp. 91–112, ISBN 978-3-030-04184-7.
32. Linsley, C.; Wu, B.; Tawil, B. The Effect of Fibrinogen, Collagen Type I, and Fibronectin on Mesenchymal Stem Cell Growth and Differentiation into Osteoblasts. *Tissue Eng. Part. A* **2013**, *19*, 1416–1423. [CrossRef]
33. Ribeiro, N.; Sousa, S.R.; Brekken, R.A.; Monteiro, F.J. Role of SPARC in Bone Remodeling and Cancer-Related Bone Metastasis: SPARC in Bone Remodeling and Bone Metastasis. *J. Cell. Biochem.* **2014**, *115*, 17–26. [CrossRef]
34. Salamanca, E.; Pan, Y.-H.; Tsai, A.; Lin, P.-Y.; Lin, C.-K.; Huang, H.-M.; Teng, N.-C.; Wang, P.; Chang, W.-J. Enhancement of Osteoblastic-Like Cell Activity by Glow Discharge Plasma Surface Modified Hydroxyapatite/β-Tricalcium Phosphate Bone Substitute. *Materials* **2017**, *10*, 1347. [CrossRef]
35. Canullo, L.; Genova, T.; Naenni, N.; Nakajima, Y.; Masuda, K.; Mussano, F. Plasma of Argon Enhances the Adhesion of Murine Osteoblasts on Different Graft Materials. *Ann. Anat.-Anat. Anz.* **2018**, *218*, 265–270. [CrossRef]
36. Gao, C.; Peng, S.; Feng, P.; Shuai, C. Bone Biomaterials and Interactions with Stem Cells. *Bone Res.* **2017**, *5*, 17059. [CrossRef]
37. Samavedi, S.; Whittington, A.R.; Goldstein, A.S. Calcium Phosphate Ceramics in Bone Tissue Engineering: A Review of Properties and Their Influence on Cell Behavior. *Acta Biomater.* **2013**, *9*, 8037–8045. [CrossRef] [PubMed]
38. Graves, D.B. The Emerging Role of Reactive Oxygen and Nitrogen Species in Redox Biology and Some Implications for Plasma Applications to Medicine and Biology. *J. Phys. D Appl. Phys.* **2012**, *45*, 263001. [CrossRef]
39. Bradu, C.; Kutasi, K.; Magureanu, M.; Puač, N.; Živković, S. Reactive Nitrogen Species in Plasma-Activated Water: Generation, Chemistry and Application in Agriculture. *J. Phys. D Appl. Phys.* **2020**, *53*, 223001. [CrossRef]
40. Lamichhane, P.; Acharya, T.R.; Kaushik, N.; Nguyen, L.N.; Lim, J.S.; Hessel, V.; Kaushik, N.K.; Choi, E.H. Non-Thermal Argon Plasma Jets of Various Lengths for Selective Reactive Oxygen and Nitrogen Species Production. *J. Environ. Chem. Eng.* **2022**, *10*, 107782. [CrossRef]
41. Stasic, J.N.; Selaković, N.; Puač, N.; Miletić, M.; Malović, G.; Petrović, Z.L.; Veljovic, D.N.; Miletic, V. Effects of Non-Thermal Atmospheric Plasma Treatment on Dentin Wetting and Surface Free Energy for Application of Universal Adhesives. *Clin. Oral. Investig.* **2019**, *23*, 1383–1396. [CrossRef] [PubMed]
42. Jeong, J.; Kim, J.H.; Shim, J.H.; Hwang, N.S.; Heo, C.Y. Bioactive Calcium Phosphate Materials and Applications in Bone Regeneration. *Biomater. Res.* **2019**, *23*, 4. [CrossRef] [PubMed]
43. Lee, D.-S.; Moriguchi, Y.; Okada, K.; Myoui, A.; Yoshikawa, H.; Hamaguchi, S. Improvement of Hydrophilicity of Interconnected Porous Hydroxyapatite by Dielectric Barrier Discharge Plasma Treatment. *IEEE Trans. Plasma Sci.* **2011**, *39*, 2166–2167. [CrossRef]
44. Humbert, P.; Brennan, M.Á.; Davison, N.; Rosset, P.; Trichet, V.; Blanchard, F.; Layrolle, P. Immune Modulation by Transplanted Calcium Phosphate Biomaterials and Human Mesenchymal Stromal Cells in Bone Regeneration. *Front. Immunol.* **2019**, *10*, 663. [CrossRef]
45. Hamlet, S.; Alfarsi, M.; George, R.; Ivanovski, S. The Effect of Hydrophilic Titanium Surface Modification on Macrophage Inflammatory Cytokine Gene Expression. *Clin. Oral. Impl. Res.* **2012**, *23*, 584–590. [CrossRef]
46. Hotchkiss, K.M.; Reddy, G.B.; Hyzy, S.L.; Schwartz, Z.; Boyan, B.D.; Olivares-Navarrete, R. Titanium Surface Characteristics, Including Topography and Wettability, Alter Macrophage Activation. *Acta Biomater.* **2016**, *31*, 425–434. [CrossRef] [PubMed]

47. Hotchkiss, K.M.; Sowers, K.T.; Olivares-Navarrete, R. Novel in Vitro Comparative Model of Osteogenic and Inflammatory Cell Response to Dental Implants. *Dent. Mater.* **2019**, *35*, 176–184. [CrossRef] [PubMed]
48. Leuning, D.G.; Beijer, N.R.M.; du Fossé, N.A.; Vermeulen, S.; Lievers, E.; van Kooten, C.; Rabelink, T.J.; Boer, J. de The Cytokine Secretion Profile of Mesenchymal Stromal Cells Is Determined by Surface Structure of the Microenvironment. *Sci. Rep.* **2018**, *8*, 7716. [CrossRef]
49. Abagnale, G.; Steger, M.; Nguyen, V.H.; Hersch, N.; Sechi, A.; Joussen, S.; Denecke, B.; Merkel, R.; Hoffmann, B.; Dreser, A.; et al. Surface Topography Enhances Differentiation of Mesenchymal Stem Cells towards Osteogenic and Adipogenic Lineages. *Biomaterials* **2015**, *61*, 316–326. [CrossRef] [PubMed]
50. Zhang, Y.; Böse, T.; Unger, R.E.; Jansen, J.A.; Kirkpatrick, C.J.; van den Beucken, J.J.J.P. Macrophage Type Modulates Osteogenic Differentiation of Adipose Tissue MSCs. *Cell Tissue Res.* **2017**, *369*, 273–286. [CrossRef] [PubMed]
51. Gamblin, A.-L.; Brennan, M.A.; Renaud, A.; Yagita, H.; Lézot, F.; Heymann, D.; Trichet, V.; Layrolle, P. Bone Tissue Formation with Human Mesenchymal Stem Cells and Biphasic Calcium Phosphate Ceramics: The Local Implication of Osteoclasts and Macrophages. *Biomaterials* **2014**, *35*, 9660–9667. [CrossRef] [PubMed]
52. Bohner, M.; Santoni, B.L.G.; Döbelin, N. β-Tricalcium Phosphate for Bone Substitution: Synthesis and Properties. *Acta Biomater.* **2020**, *113*, 23–41. [CrossRef] [PubMed]
53. Viti, F.; Landini, M.; Mezzelani, A.; Petecchia, L.; Milanesi, L.; Scaglione, S. Osteogenic Differentiation of MSC through Calcium Signaling Activation: Transcriptomics and Functional Analysis. *PLoS ONE* **2016**, *11*, e0148173. [CrossRef]
54. Tour, G.; Wendel, M.; Tcacencu, I. Bone Marrow Stromal Cells Enhance the Osteogenic Properties of Hydroxyapatite Scaffolds by Modulating the Foreign Body Reaction: BMSCs Modulate Foreign Body Reaction. *J. Tissue Eng. Regen. Med.* **2014**, *8*, 841–849. [CrossRef]